Author's response to the Reviewers' comments

Please refer to the detailed itemized responses below. Our responses are indicated in blue text and the text referring to the clean version is indented. Edits compared to the last version are highlighted in red text.

Response to Reviewer #1

This manuscript presents a modelling study using the CliMA land surface model investigating the effect of assumptions around tree recovery after drought at one site which experienced a severe drought in 2012. The results show that including a mechanism for partial rather than full recovery leads to a better fit to data in the post-drought period. This is an important topic as models still frequently assume instantaneous responses to environmental conditions and there is no standard framework for representing lagged responses.

In general, the analysis is scientifically sound but the paper itself need some edits to make it more robust and easier to understand.

[Response]

We thank the reviewer for their constructive feedback. In response, we have expanded the Methods section to provide details on variable definitions and their computation. We have also clarified the model configurations and the reasons for their different performance. All other line-by-line comments have been carefully addressed. We believe these revisions adequately address the reviewer's concerns.

Major comments

The methods are poorly written, with concepts that are not explained, variables that are not defined and inconsistency between notations (detailed comments below). The whole section needs to be re-written to allow the reader to understand what was actually done more easily

[Response]

We thank the reviewer for pointing this out and apologize for the lack of clarity in the original manuscript. To address this issue, we have (1) explicitly described the calculation of key variables, particularly those involved in the three recovery scenarios; (2) added descriptions of the additional flux-tower sites used in the model simulations in Methods; and (3) ensured that notation is used consistently throughout the manuscript. Please see revised Methods in clean version.

There is a lot of stress on the differences between the full and partial recovery representations, which is interesting and relevant, but very little emphasis on the three different stomatal models presented. In most cases there don't seem to be that many differences between the three, with the exception of the model fit for the partial recovery (Fig. 5) some more explanations are needed here.

[Response]

We thank the reviewer for pointing this out. Applying β to V_{cmax} represents a biochemical limitation, directly reducing photosynthetic capacity and indirectly constraining stomatal conductance via reduced assimilation. This leads to a stronger and more persistent reduction in GPP, with comparatively weaker impacts on transpiration. In contrast, applying β to g1 represents a non-biochemical (stomatal) limitation, directly reducing stomatal conductance and CO_2 diffusion, thereby suppressing transpiration and secondarily reducing photosynthesis. As a result, when model performance of transpiration is similar between the two setups, as in the FR scenario, where transpiration is used to constrain K_{max}, photosynthesis simulated by the Medyn-g1 tends to be slightly higher than that from the Medlyn-V_{cmax} configuration (Figure 5b, 5c). Similarly, under the PR scenario, reducing the overestimation of carbon fluxes is accompanied by an underestimation of transpiration (Figure 5c, 5f). In the optimality-based stomatal model, β acts on hydraulic conductance only, and thus affects stomatal conductance indirectly, resulting in a response similar to the Medlyn-g1 formulation and a comparable underestimation of transpiration.

To address this issue, we added further explanation in lines 325-334 in the clean version.

> Applying β to V_{cmax} represents a biochemical limitation, directly reducing photosynthetic capacity and indirectly constraining stomatal conductance via reduced assimilation. This leads to a stronger and more persistent reduction in GPP, with comparatively weaker impacts on transpiration. In contrast, applying β to g1 represents a non-biochemical (stomatal) limitation, directly reducing stomatal conductance and CO_2 diffusion, thereby suppressing transpiration and secondarily reducing photosynthesis. As a result, when model performance of transpiration is similar between the two setups, as in the FR scenario, where transpiration is used to constrain K_{max}, photosynthesis simulated by the Medyn-g1 tends to be slightly higher than that from the Medlyn-V_{cmax} configuration (Figure 5b, 5c). Similarly, under the PR scenario, reducing the overestimation of carbon fluxes is

accompanied by an underestimation of transpiration (Figure 5c, 5f). In the optimality-based stomatal model, β acts on hydraulic conductance only, and thus affects stomatal conductance indirectly, resulting in a response similar to the Medlyn-g1 formulation and a comparable underestimation of transpiration.

The partial recovery is implemented by fitting the model to observations rather than through a process based representation. This raises two questions. First – how general is this method? Can the model make predictions at sites where there is no eddy covariance data? Second – how much is the improvement in fit after the introduction of partial recovery to do with partial recovery itself and how much is it to do with the fact that the model is brought closer to observations via data assimilation?

[Response]

We thank the reviewer for pointing this out. Regarding generalizability, the proposed method can be applied at sites with eddy-covariance observations to derive general constraints on vegetation recovery processes, which can then be transferred to sites lacking eddy-covariance measurements. For example, key recovery characteristics, such as the time required for the release of accumulated water deficit and the upper bound of hydraulic conductance recovery, can be derived from existing eddy-covariance observations. These features can then be related to commonly available environmental variables using nonlinear regression or machine-learning approaches, enabling their prediction at sites without eddy-covariance data. This clarification has been added in the lines 449-456 in the clean version.

This site-level research lays the groundwork for potential regional expansions to delve further into the factors influencing drought recovery and to validate the generalizability of the identified responses. Specifically, the proposed approach can be applied at sites with eddy-covariance observations to derive general constraints on vegetation recovery processes, which can then be extended to sites lacking such measurements. For example, key recovery characteristics, such as the time required for the release of accumulated water deficit and the upper bound of hydraulic conductance recovery, can be inferred from flux tower data. These features can subsequently be linked to commonly available environmental variables using nonlinear regression or machine-learning approaches, enabling their prediction across broader spatial domains without eddy-covariance coverage.

In this framework, partial recovery involves two components: (1) the introduction of a partial recovery process in the model, and (2) data assimilation to infer the upper bound to which the hydraulic system can recover. To investigate the model improvement with introduction of a partial recovery process, we impose a constraint whereby vegetation is allowed to recover only to 80% of the full-recovery condition or leaf water potential can only recover to -3 MPa as the maximum, which are treated as A1 and A2 (partial recovery alone), and compare it with A3, which additionally includes data assimilation. By comparing model performance between A1, A2 and A3 (Figures R1-R3), we find that the improvement associated with partial recovery is primarily driven by the data assimilation component.

To further clarify the improvement brought by the partial recovery setup, we added below text into the clean version as lines 318-319.

> We found that introducing a partial recovery setup with a fixed bound is inadequate to capture the post-drought responses of carbon and water fluxes, necessitating the data assimilation of using observations as constraint (Figure S5, S6).

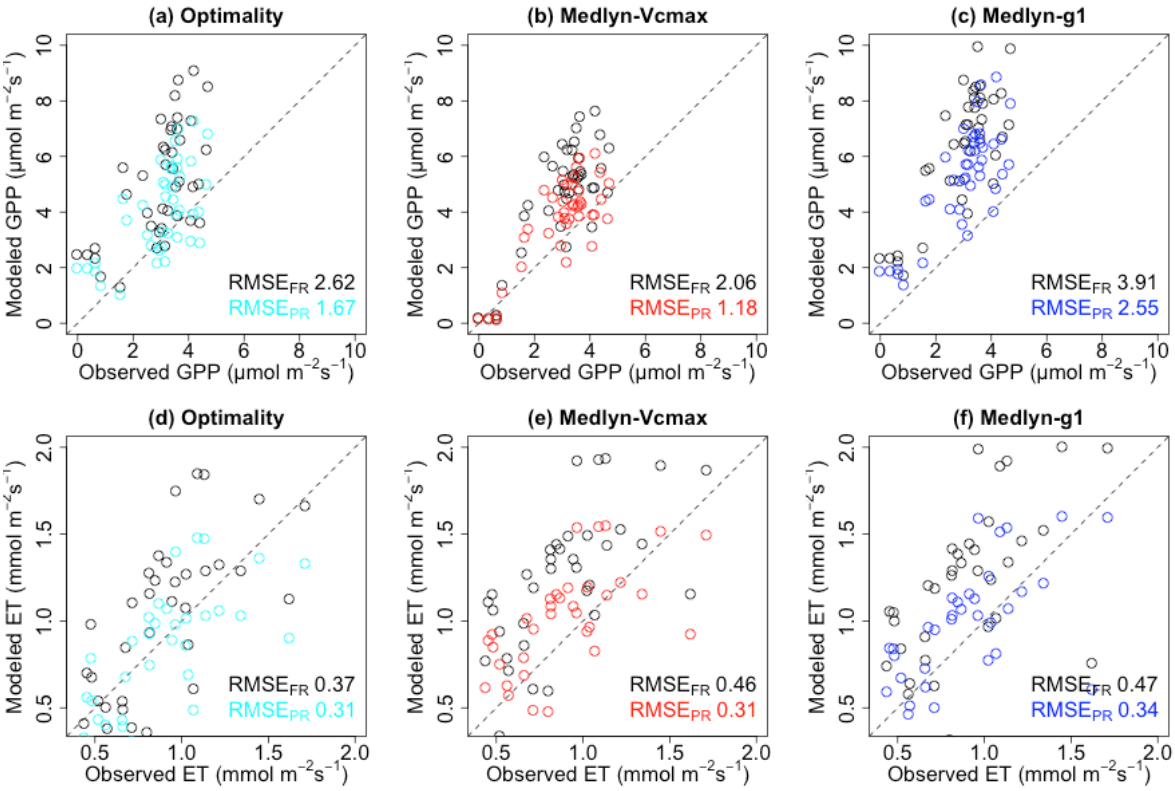

Figure R1 Change in model performance after accounting for drought legacy effects by setting recovery upper boundary to 80% of the full-recovery condition (recovery period only).

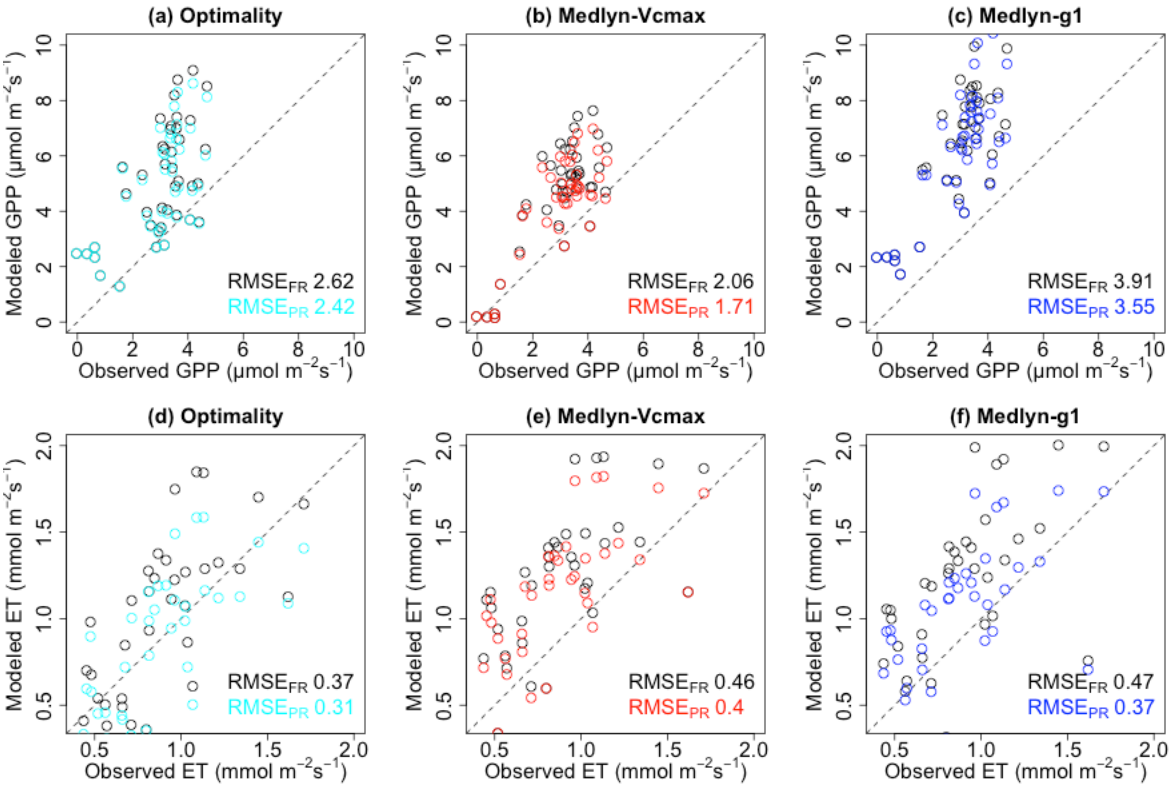

Figure R2 Change in model performance after accounting for drought legacy effects by setting recovery upper boundary to -3 MPa of leaf water potential (recovery period only).

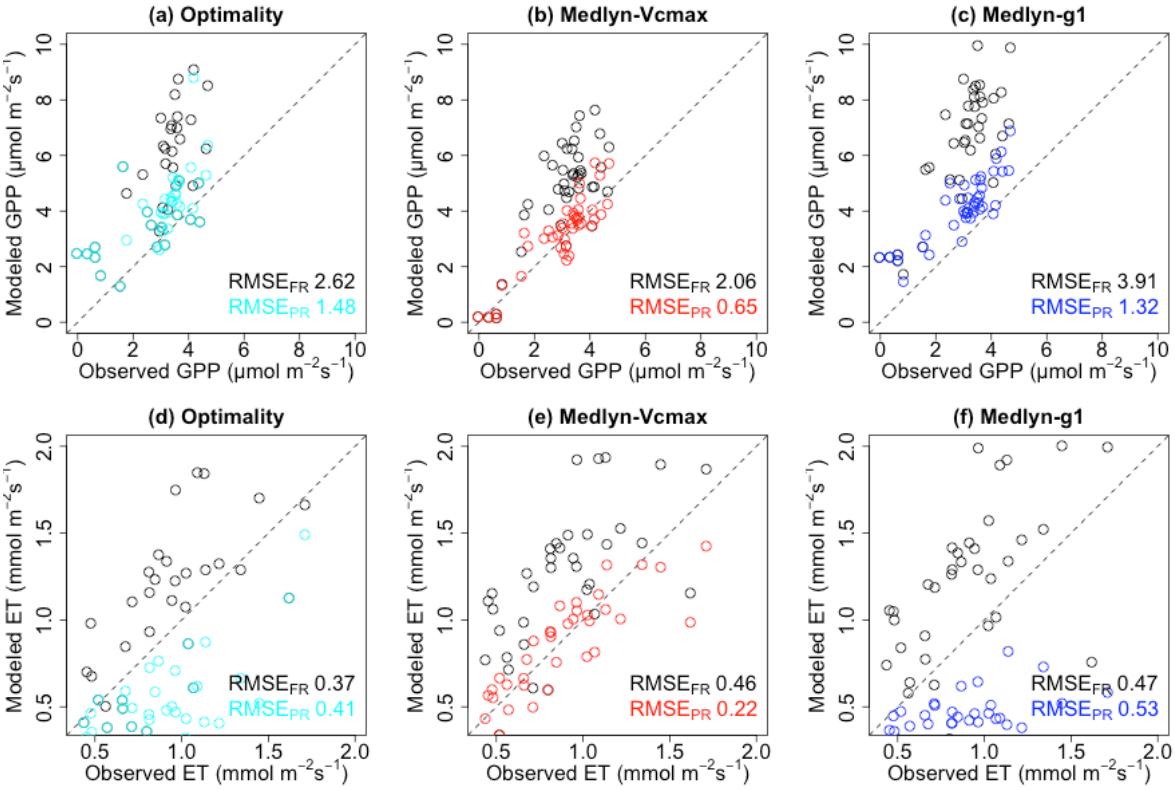

Figure R3 Change in model performance after accounting for drought legacy effects by data assimilation (recovery period only).

Minor comments

L 135 does the MODIS LAI respond to drought at the site? Does having this as an input partially represent the effects of drought already?

[Response]

Yes, MODIS LAI decreased in response to the 2012 drought (Figure R4). We therefore consider that using MODIS LAI as an input already captures canopy structural responses to drought. MODIS LAI time series is shown as Figure S1 in SI.

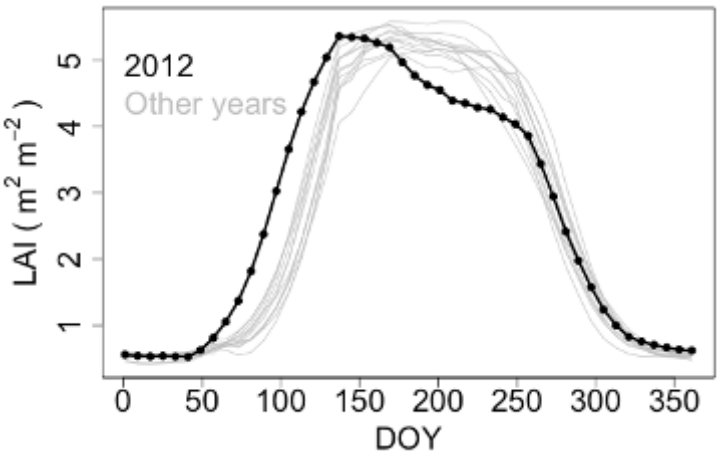

Figure R4 LAI time series in 2012 extracted from MODIS LAI products using GriddingMachine package (Wang et al., 2022; Yuan et al., 2011).

L 150 unclear why, given the research questions, it is necessary to evaluate canopy spectra

[Response]

We now remove the evaluation of canopy spectra.

L 167 "Changing this T/ET ratio does not impact our results." Some evidence is needed here

[Response]

To avoid potential evaluation bias associated with assuming a fixed T/ET ratio, we applied the ET partitioning method of Nelson et al. (2020) to directly compare modeled transpiration with observation-based partitioned transpiration. This partitioning approach allows the T/ET ratio to vary dynamically. We find that using either a fixed T/ET ratio or observation-based partitioned transpiration does not alter our conclusions, namely, that biochemical limitations delay the recovery of both carbon and water fluxes (Figures R5, R6).

To address this issue, the corresponding figures (Figures S9, S10) have been added to SI and we have added below sentences in the clean version.

Lines 157-158 in Methods:

> We also tested varying T/ET ratio with observation-based partitioned transpiration (Nelson et al., 2020).

Lines 339-343 in Results:

Instead of relying solely on a fixed T/ET ratio, we applied the ET partitioning approach of Nelson et al. (2020) to directly compare modeled transpiration with observation-based partitioned transpiration. This method allows the T/ET ratio to vary dynamically. We find that using either a fixed T/ET ratio or observation-based partitioned transpiration does not affect our conclusions, namely, that biochemical limitations delay the recovery of both carbon and water fluxes (Figures S9, S10).

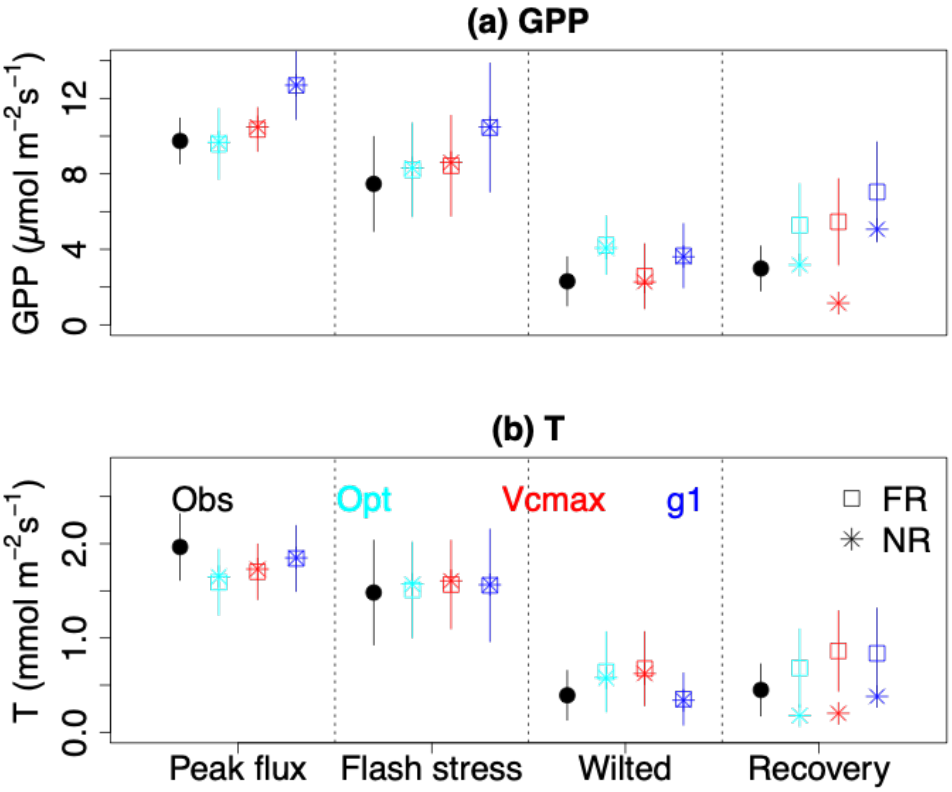

Figure R5 Model performance for GPP and T across four periods in 2012. Curves show the optimality-based stomatal model (cyan) and the Medlyn model with the water-stress factor applied to Vcmax (red) or to g1 (blue). FR, full recovery; NR, no recovery. Error bars indicate variability within each period.

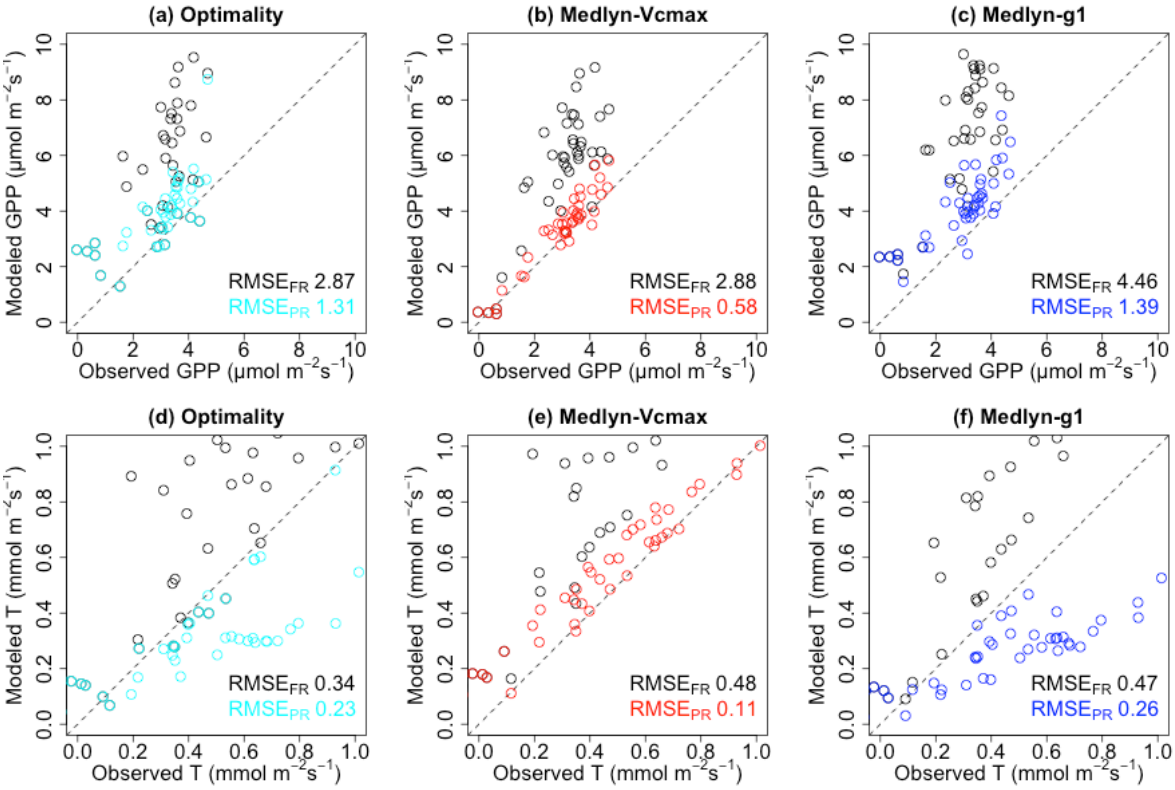

Figure R6 Improvement in model performance after accounting for drought legacy effects (recovery period only). Scatterplots compare RMSE under the partial-recovery scenario ($RMSE_{PR}$) against the full-recovery baseline ($RMSE_{FR}$) for GPP and T. Symbols denote simulations assuming full recovery (black circles) and partial recovery using the optimality-based model (cyan) or the Medlyn model with the water-stress factor applied to Vcmax (red) or g1 (blue). RMSEs are computed against flux observations; lower values indicate better fit.

L 167 "The CliMA Land model was employed to reproduce the dynamics of carbon and water fluxes during the drought period." This statement feels superfluous here.

[Response]

We will remove this sentence.

L 171 "several stomatal optimality models" sever feels very vague here

[Response]

To address this issue, this sentence has been revised as:

The CliMA Land model incorporates several stomatal optimality models (e.g., Eller et al., 2018, Sperry et al., 2017, Wang et al., 2020) and three empirical stomatal models: the Medlyn (Medlyn et al., 2011), Ball-Berry (Ball et al., 1987) and Leuning models (Leuning, 1995).

L 189 table 1 – this table has only 1 line, but above you say you also used an optimal model

[Response]

Because β factor does not directly affect V_{cmax} or stomatal conductance in the optimality-based stomatal model, it was not included in Table 1. To solve this issue, we showed the equations for Medlyn-V_{cmax} and Medlyn-g1 and removed the Table 1.

Section 2.4 – many more details are needed here, preferably in the form of equations. It is not enough to say that vulnerability curves or the data assimilation method is taken from another paper

[Response]

We apologize for the unclear description. The equations describing the three recovery scenarios are provided below and have been added into the revised version.

Full recovery scenario (FR): Hydraulic conductance can either increase or decrease and the shape of the vulnerability curve remains constant, i.e. is not affected by the previous severe water stress condition. In other words, the water potential and hydraulic conductance can be updated without specific boundaries (Eq. 9). Only transient (or immediate) responses are considered.

$K^{FR}(t)$ is updated according to the water stress factor β (Eq. 9).

$$K^{FR}(t) = K_{max} \cdot \beta(\psi(t)) \quad \text{Eq. (9)}$$

$\psi(t)$ is leaf water potential at time t. $K^{FR}(t)$ is hydraulic conductance under FR at time t.

Partial recovery scenario (PR): In reality, the full recovery of the hydraulic system may not necessarily occur due to irreversible processes such as a broken hydraulic transport system (e.g., embolism). Recovery can vary depending on the time scale; for instance, the construction of new xylem over time may facilitate greater recovery, while immediate recovery following a drought may be limited. The extent of potential plant recovery can be inferred from the response of carbon and water fluxes to post-drought climate conditions

by applying a similar concept of optimizing ecosystem models through assimilating eddy-covariance measurements in Wolf et al. (Wolf et al., 2006). By minimizing the difference between modeled and observed carbon and water fluxes, we diagnostically derived the water stress time series and updated modeled leaf water potential at each time step. β is estimated by minimizing the model-observation mismatch (Eq. 10). $K^{PR}(t)$ is then updated using the inverted β (Eq. 11).

$$\beta^*(t) = \arg\min_{\beta\in[\beta_{min},1]} \sum_t \left\{ \left[\frac{GPP_{mod}(t;\beta) - GPP_{obs}(t)}{SD(GPP_{obs})} \right]^2 + \left[\frac{ET_{mod}(t;\beta) - ET_{obs}(t)}{SD(ET_{obs})} \right]^2 \right\} \quad \text{Eq. (10)}$$

$$K^{PR}(t) = K_{max} \cdot \beta^*(t) \quad \text{Eq. (11)}$$

$K^{PR}(t)$ is hydraulic conductance under PR at time t.

In empirical stomatal models, β serves as an integrated proxy for the recovery state of both hydraulic and biochemical or stomatal processes, and their dynamics jointly contribute to the simulated drought legacy effects. Comparing Medlyn-V_{cmax} and Medlyn-g1 configurations reveals which process, biochemical or nonbiochemical, better explains the recovery of carbon and water fluxes.

No recovery scenario (NR): Hydraulic conductance can't increase (recover) over time. During severe water stress events, hydraulic conductance decreases due to a drop in water potential. Subsequently, during the post-drought period, hydraulic conductance cannot increase or return to its pre-drought state. $K^{NR}(t)$ is constrained to be non-increasing (Eqs. 12-13). When drought causes ψ(t) to become more negative, instantaneous hydraulic conductance K^{inst} drops and K^{NR} drops. After drought, ψ(t) becomes less negative and K^{inst} increases. However, the minimum operator in Eq. (13) prevents recovery of K^{NR}.

$$K^{inst}(t) = K_{max} \cdot \beta(\psi(t)) \quad \text{Eq. (12)}$$

$$K^{NR}(t) = \min\left(K^{NR}(t-1), K^{inst}(t)\right) \quad \text{Eq. (13)}$$

where $K^{NR}(t)$ is hydraulic conductance under NR at time t.

All three recovery scenarios share the same initial condition corresponding to the pre-drought state (Eq. 14).

$$K^{FR}(t_0) = K_{max} \cdot \beta(\psi(t_0)) \quad \text{Eq. (14)}$$

where t_0 represents time before recovery.

L 215 Table 2 – unclear what information this table add as everything is just a tick. The notations for the two options for the Medlyn model also do not match those in Table 1

[Response]

In the previous version, this table was included to indicate that a total of nine scenarios were considered, arising from three stomatal model configurations combined with three recovery scenarios. As the table provides limited additional information, we have removed it from the revised manuscript.

L 231 what is Kmax? Seems like an important parameter but it is the first time it's mentioned I think

[Response]

We apologize for the missing description. K_{max} denotes the maximum hydraulic conductance.

L 257 is this the same method as the data assimilation for the partial recovery scenario above or something else?

[Response]

Yes. We used this equation as an error function during data assimilation. It has been merged into Eq. 10 as:

$$\beta^*(t) = \arg\min_{\beta\in[\beta_{min},1]} \sum_t \left\{ \left[\frac{GPP_{mod}(t;\beta) - GPP_{obs}(t)}{SD(GPP_{obs})} \right]^2 + \left[\frac{ET_{mod}(t;\beta) - ET_{obs}(t)}{SD(ET_{obs})} \right]^2 \right\} \quad \text{Eq. (10)}$$

L 335 But the model overestimates the coupling during the wilted period as well, so the issue here is not just the full recovery assumption

[Response]

We agree that the model overestimates the coupling strength during both the wilted and recovery period. Here, through the comparison of GPP-ET coupling coefficient derived from flux data among four periods, it shows that non-stomatal limitations occur during the drought and persists into the recovery period. We also acknowledge that model simulations overestimate this coupling strength in both drought and recovery periods. This could be due to the explicit linkage between GPP and transpiration through stomatal conductance in our model setup.

To address this issue, we revised this sentence as:

The weaker GPP-ET coupling derived from flux observations indicates the emergence of non-stomatal limitations during drought, which can persist into the recovery phase. In contrast, model simulations tend to overestimate this coupling, likely because GPP and transpiration are tightly linked through stomatal conductance.

L 338 this looks like a repetition of the methods here

[Response]

We have removed this paragraph.

L 346 it might help here to show a timeseries of model GPP and ET to understand the evolution of recovery

[Response]

We agree. Below we show the time series of modeled GPP and ET (Figure R7). This has been added into SI as Figure S7. Please see lines 320-321 in clean version.

After assimilating flux observations as constraints, we observed a slower alleviation of water stress compared to the full recovery assumption and a similarly delayed increase in carbon fluxes (Figure S7, S8).

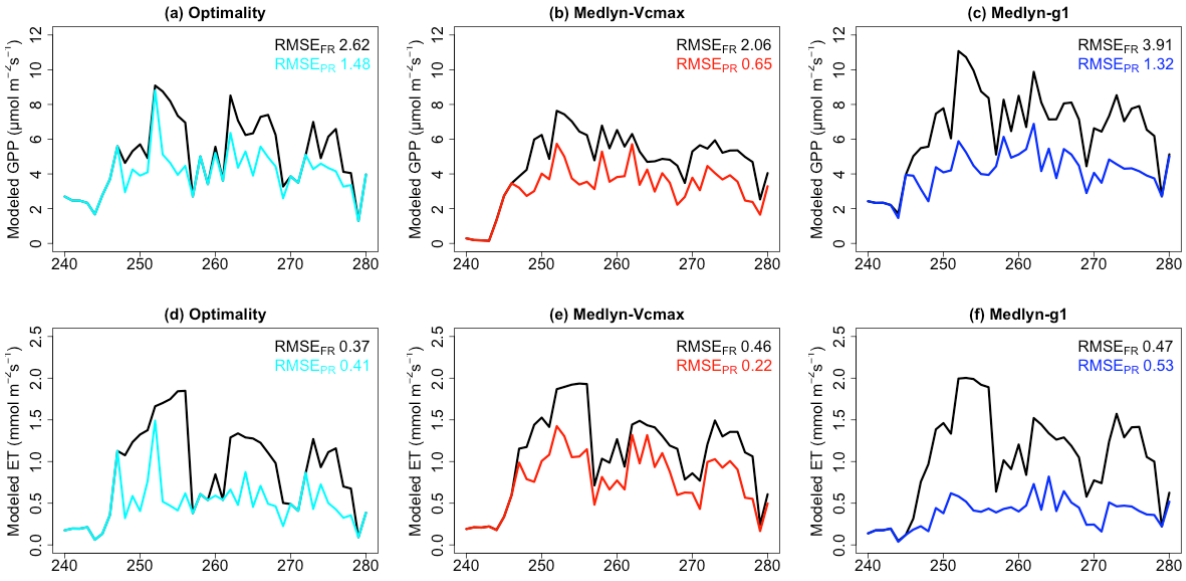

Figure R7 Time series of GPP and ET during recovery period between FR and PR.

L 421 it feels odd to mention simulations at other sites in the discussion for the first tiem when this was not mentioned in the methods

[Response]

To address this issue, we have added descriptions of the additional validation sites in the Methods, as shown below.

2.2 Other flux sites used for model validation

We conducted model simulations at several flux-tower sites that experienced the 2012 drought, including US-MMS, US-GLE, US-UMB, US-NR1, and US-UMd. The US-MMS site is located in Morgan-Monroe State Forest, Indiana, within a temperate deciduous broadleaf forest dominated by a maple–beech–oak–hickory transition community representing secondary successional stands approximately 60–80 years old (Novick and Phillips, 2022). The US-GLE site is located in northern Michigan and consists of a mixed forest composed of aspen, maple, pine, and northern hardwood species (Frank et al., 2022). The US-UMB site, also located in northern lower Michigan, is an aspen-dominated northern hardwood forest (FLUXNET2015). The US-NR1 site is located in the Rocky Mountains of Colorado within a subalpine evergreen needleleaf forest dominated by *Abies lasiocarpa*, *Picea engelmannii*, and *Pinus contorta* (FLUXNET2015). The US-UMd site, located in northern lower Michigan, represents a temperate deciduous broadleaf forest (Gough et al., 2024).

References

Frank John, Valentine George, Massman Bill (2022), AmeriFlux FLUXNET-1F US-GLE GLEES, Ver. 3-5, AmeriFlux AMP, (Dataset). https://doi.org/10.17190/AMF/1871136

Gough Christopher, Bohrer Gil, Curtis Peter (2024), AmeriFlux FLUXNET-1F US-UMd UMBS Disturbance, Ver. 4-6, AmeriFlux AMP, (Dataset). https://doi.org/10.17190/AMF/1881597

Novick Kim and Phillips Rich (2022). AmeriFlux FLUXNET-1F US-MMS Morgan Monroe State Forest. (Dataset) https://doi.org/10.17190/AMF/1854369

Response to Reviewer #2

In this manuscript, Yao et al. examine drought legacy effects on carbon and water fluxes using eddy-covariance observations and a process-based model for a temperate forest in the central US. The manuscript is generally well written and reflects considerable effort in the model experiments and data analysis. It has the potential to contribute to the literature by providing a data–model fusion framework for understanding drought legacy effects and improving the representation of post-drought recovery of carbon and water fluxes. I only have several concerns that should be addressed before publication.

[Response]

We thank the Reviewer for the positive feedback on our study. In response, we have expanded the Methods section to provide a clearer description of the model structure and the derivation of key variables. We have also tested the robustness of our conclusions by using observation-based partitioning of transpiration (T/ET). In addition, we have further elaborated on the roles of downregulation of V_{cmax} and loss of hydraulic conductance in shaping drought legacy effects. All other line-by-line comments have also been addressed. We believed these revisions effectively address the concerns raised by the Reviewer.

Major comments:

1) The overall structure of the methodology is understandable, but some key details are missing. The equations for how GPP, ET, leaf water potential, and hydraulic conductance are calculated should be included. They are important for readers to understand how the water stress factor affects the dynamics of these variables.

[Response]

We thank the Reviewer for pointing this out. The calculations of key variables, including GPP, transpiration, leaf water potential, and hydraulic conductance, are summarized below. To address this issue, we have incorporated these descriptions into the revised Methods.

Leaf-level photosynthesis is solved by coupling the diffusion model with the Farquhar model (Eq .1).

$$A_{net} = V_{cmax}\frac{C_i - \Gamma^*}{C_i + K_m} - R_d = g_s \cdot (C_a - C_i) \quad \text{Eq. (1)}$$

where V_{cmax} is the maximum rate of Rubisco activity and K_m is the Michaelis-Menten coefficient for Rubisco kinetics. Γ^* is the CO_2 compensation point in the absence of dark respiration and R_d

is the dark respiration rate. C_i is the intercellular CO_2 concentration. The model details of stomatal conductance (g_s) can be found in Section 2.4.

Canopy transpiration is computed using the diffusion model as Eq. 2.

$$T = \sum_{i=1}^{n_{canopy}} 1.6 \cdot g_s \cdot D \cdot LAI_i \quad \text{Eq. (2)}$$

LAI_i is the leaf area index of i^{th} layer. D is leaf-to-air vapour pressure deficit. 1.6 is the unitless relative diffusivity of water vapor with respect to CO_2.

Leaf water potential (Ψ_{leaf}) is updated following Darcy's law based on vertical water flow and hydraulic conductance (Eq. 3).

$$\psi_{leaf} = \psi_{soil} - F \times \sum_{i \in leaf,stem,root} \frac{1}{K_i} \quad \text{Eq. (3)}$$

F is transpiration-driven vertical water flow and K_i is hydraulic conductance of each segment. Ψ_{soil} is soil water potential.

In empirical formulations, drought responses are introduced through a water stress factor β. Two pathways of stress propagation are considered. The first one operates by adjusting parameters of the empirical stomatal models, such as the slope parameter (g1) (Eq. 4). The second pathway involves the modulation of photosynthetic capacity through down-regulation of V_{cmax} (Eq. 5), which also reduces stomatal conductance as photosynthesis is reduced.

$$g_s = g_0 + \beta \cdot \left(1 + \frac{g_1}{\sqrt{D}}\right) \cdot \frac{A_{net}}{C_a} \quad \text{Eq. (4)}$$

$$g_s = g_0 + \left(1 + \frac{g_1}{\sqrt{D}}\right) \cdot \frac{A_{net}(\beta)}{C_a} \quad \text{Eq. (5)}$$

where C_a is the atmospheric CO_2 concentration. D is leaf-to-air vapour pressure deficit. g_0 and g_1 are empirical parameters.

For the optimality-based model, stomatal conductance maximizes the difference between leaf-level carbon gain and hydraulic risk, with risk represented through leaf hydraulics and their coupling to photosynthesis (Eq. 6).

$$g_s = \text{argmax}\left(A_{net} - A_{net}\frac{E}{E_{crit}}\right) \quad \text{Eq. (6)}$$

where E is the leaf-level transpiration rate, and E_{crit} is the critical transpiration rate at which the leaf xylem hydraulic conductance decreases to 0.1% of the maximum value (namely at 99.9% loss of hydraulic conductance). A_{net} is the net photosynthesis rate.

Hydraulic conductance (K) is updated following the Weibull function (Eq. 7).

$$K = K_{max} \cdot e^{-1 \cdot \left(\frac{-\psi}{b}\right)^c} \quad \text{Eq. (7)}$$

K_{max} is maximum hydraulic conductance. b and c are empirical parameters. ψ is leaf water potential.

2) The authors show the comparison of GPP and ET between observations and model simulations under different scenarios across drought stages in an aggregated way. It would be great to show the temporal dynamics in more detail by showing the daily time series, which could help convey the messages more clearly to readers. In addition, the time series of the water stress and hydraulic conductance under the partial recovery scenario could be worth showing to demonstrate the role of the partial recovery of hydraulic conductance in the recovery of carbon and water fluxes.

[Response]

We thank the Reviewer for pointing this out. We have added time series of GPP and ET (Figure R1) and showed how water stress recovers under the partial recovery scenario (Figure R2). To address this comment, time series of GPP and ET have been shown as Figure S2 in SI and mentioned in lines 271-272 in clean version.

> All tested stomatal schemes from CliMA Land demonstrated their ability to capture seasonal variations in carbon and water fluxes during the growing season of 2012 under the assumption of full recovery (Figure 3, S2).

Time series of water stress has been added as Figure S8 in SI and mentioned in lines 320-321 in the revised clean version.

> After assimilating flux observations as constraints, we observed a slower alleviation of water stress compared to the full recovery assumption and a similarly delayed increase in carbon fluxes (Figure S7, S8).

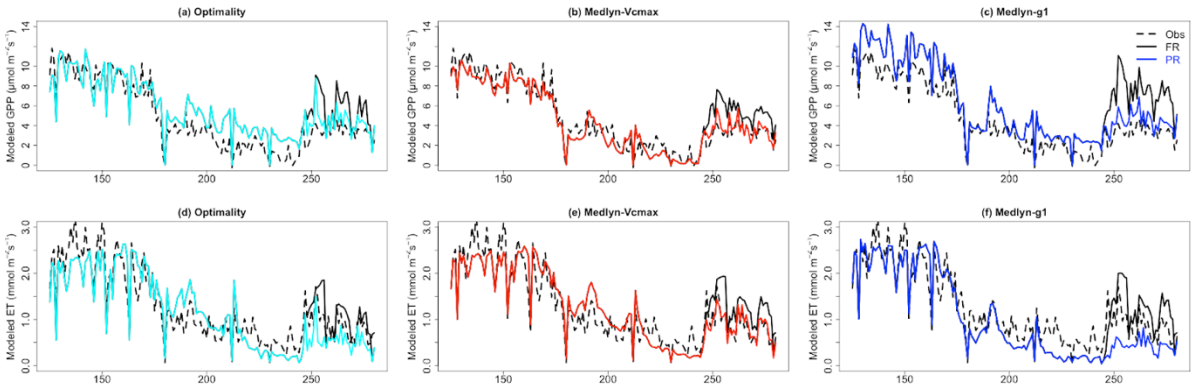

Figure R1 Time series of GPP and ET between observations and model simulations. FR: full recovery. PR: partial recovery.

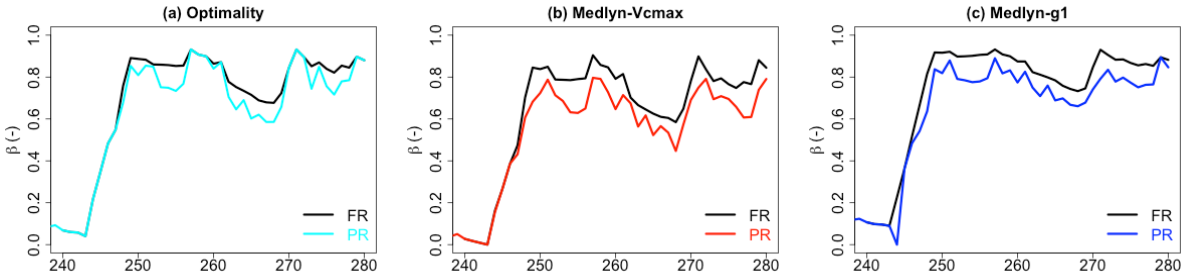

Figure R2 Time series of water stress (β) under the full recovery (FR) and partial recovery (PR) scenarios.

3) Because the model does not simulate soil evaporation and re-evaporation of rainfall interception, the authors assume a fixed T/ET ratio to link transpiration (T) to observed ET. However, this is a strong assumption in the context of drought legacy effects on ET. Because, given the same conditions of water and energy availability, the reduced T due to legacy effects could be compensated by the soil evaporation, resulting in a similar magnitude of ET. Therefore, the result that the ET simulation under the full-recovery assumption is closer to the observation than the non-recovery assumption could be confounded by this compensation effect. This could also question the finding that a quicker resumption of ET, but a slower recovery of GPP. Given that the model used can not simulate soil evaporation, I suggest authors try to use an ET partitioning method (e.g., Nelson et al., 2020) to estimate transpiration and directly compare it with model simulations.

[Response]

Following the Reviewer's suggestions, we used the uWUE method from Nelson et al. (2020) for ET partitioning and compared the partitioned T against model simulations.

Method description

$$uWUE = \frac{GPP \cdot \sqrt{D}}{ET} \quad \text{Eq. (1)}$$

The potential uWUE (uWUEp) is calculated at an annual scale using a 95th percentile regression between $GPP \cdot \sqrt{D}$ and ET (Eq. 1), representing the conditions with the highest carbon gain to

water loss and thus T = ET. The apparent uWUE (uWUEa) is estimated directly from Eq. 2 when estimating at half-hourly resolution.

$$\frac{T}{ET} = \frac{uWUE_a}{uWUE_p} \quad \text{Eq. (2)}$$

Using the partitioned transpiration (T) as the observation constraint, we find model simulations overestimate the recovery of both T and GPP (Figure R3). After applying the partial recovery setup, we find that it is still incorporating biochemical limitations (Medlyn-V_{cmax} setup) that yields the minimum model-observation mismatch (Figure R4).

To address this comment, below sentences have been added into lines 339-343 in the clean version.

> Instead of relying solely on a fixed T/ET ratio, we applied the ET partitioning approach of Nelson et al. (2020) to directly compare modeled transpiration with observation-based partitioned transpiration. This method allows the T/ET ratio to vary dynamically. We find that using either a fixed T/ET ratio or observation-based partitioned transpiration does not affect our conclusions, namely, that biochemical limitations delay the recovery of both carbon and water fluxes (Figures S9, S10).

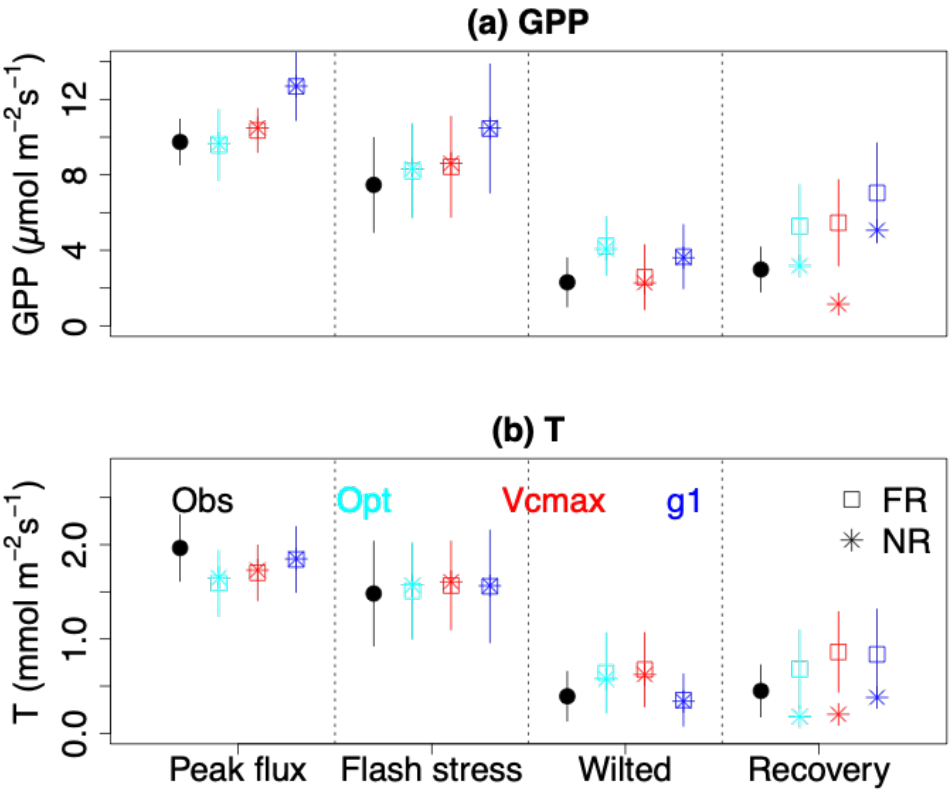

Figure R3 Model performance for GPP and T across four periods in 2012. Curves show the optimality-based stomatal model (cyan) and the Medlyn model with the water-stress factor applied to Vcmax (red) or to g1 (blue). FR, full recovery; NR, no recovery. Error bars indicate variability within each period.

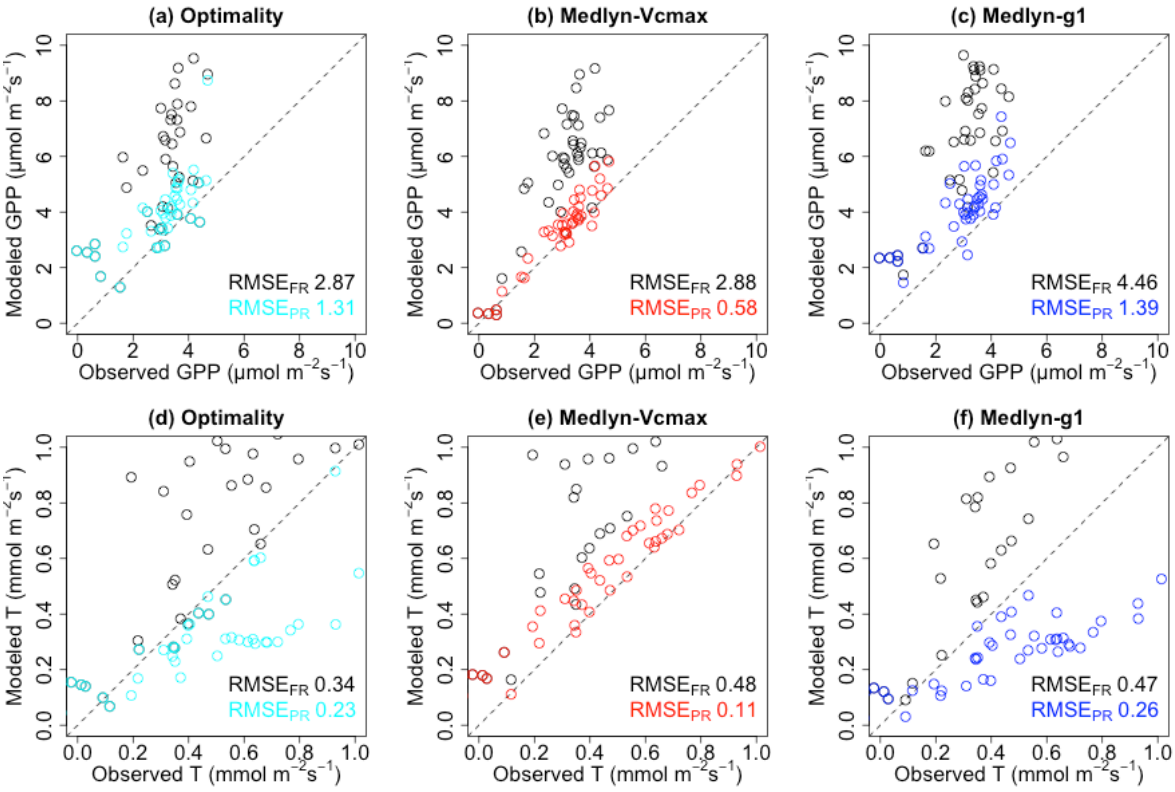

Figure R4 Improvement in model performance after accounting for drought legacy effects (recovery period only). Scatterplots compare RMSE under the partial-recovery scenario ($RMSE_{PR}$) against the full-recovery baseline ($RMSE_{FR}$) for GPP and T. Symbols denote simulations assuming full recovery (black circles) and partial recovery using the optimality-based model (cyan) or the Medlyn model with the water-stress factor applied to Vcmax (red) or g1 (blue). RMSEs are computed against flux observations; lower values indicate better fit.

4) I am a little confused about the true mechanisms investigated in this study. The authors design three hydraulic conductance recovery scenarios and use a water stress factor (β), which gives the impression that the effect of partial recovery of hydraulic conductance is examined. However, in the analysis, this β factor is used to adjust Vcmax to account for the down-regulation of photosynthetic capacity, and in the discussion later, the significance of Vcmax impairment in

shaping the delayed recovery of carbon fluxes is highlighted. Is the down-regulation of photosynthetic capacity the consequence of the loss of hydraulic conductance? Or they jointly contribute to drought legacy effects. There seems to be a mixture of these two processes. It would be great if this point could be clarified throughout the manuscript.

[Response]

We thank the Reviewer for pointing this out and apologize for the lack of clarity.

In our modeling framework, the downregulation of photosynthetic capacity is linked to the loss of hydraulic conductance through the water stress factor (β). Unlike conventional approaches where β is prescribed as an empirical function of soil moisture, here β is derived from changes in hydraulic conductance, thereby providing a mechanistic link between hydraulic status and physiological responses. To account for delayed recovery of biochemical limitations, we introduce a recovery trajectory by inverting β, which imposes a lagged recovery of hydraulic conductance and, consequently, photosynthetic capacity. In the Medlyn–V_{cmax} configuration, β directly scales V_{cmax}, whereas in Medlyn–g1 it modifies stomatal sensitivity. Overall, β serves as an integrated proxy for the recovery state of both hydraulic and biochemical (or stomatal) processes, and their dynamics jointly contribute to the simulated drought legacy effects. Comparison of the Medlyn–V_{cmax} and Medlyn–g1 configurations indicates that V_{cmax} downregulation better explains the observed recovery patterns of carbon fluxes. To address this comment, we have clarified this point in revised clean version as below:

Lines 227-230 in Methods:

> In empirical stomatal models, β serves as an integrated proxy for the recovery state of both hydraulic and biochemical (or stomatal) processes, and their dynamics jointly contribute to the simulated drought legacy effects. Comparing Medlyn-V_{cmax} and Medlyn-g1 configurations reveals which process, biochemical or nonbiochemical, better explains the recovery of carbon and water fluxes.

Lines 402-403 in Discussion:

> Based on our tests of legacy detection methods, this study underscores the significance of V_{cmax} impairment in shaping delayed recovery of carbon fluxes, with hydraulic stress being jointly considered in drought legacy effect.

Lines 477-479 in Conclusion:

To address this limitation, we introduced a progressive biochemical recovery process into the model diagnostically, accounting for both delayed hydraulic recovery and impairment of Rubisco activity.

Line-by-line comments:

Line 4: repeated numbers

[Response]

We removed the number.

Line 23: timing? You mean duration?

[Response]

Yes. This sentence is rephrased as:

Further research to mechanistically represent dynamic recovery processes, particularly their duration and magnitude, is essential for improving the modeling of global carbon and water fluxes.

Line 35: From my understanding, Ciais et al. (2005) did not include legacy effects. Also, it is unclear if drought legacy effects could shift ecosystems from carbon sinks to carbon sources. Maybe consider rephrasing this sentence.

[Response]

We rephrased this part as:

This lagged recovery, often referred to as the drought legacy effect, has been documented in drought-induced tree mortality (Matusick et al. 2018), carbon fluxes (Haberstroh et al. 2025), and tree ring growth (Anderegg et al., 2015).

Line 149: Where is Figure S1? The entire supplement seems to be missing.

[Response]

We apologize for missing SI. We will upload SI during the revision stage.

Lines 172-173: It would be great if the equation of the optimality stomatal model or more details could be provided. How to apply β to it?

[Response]

We have added the equation and explanation in the revised version in lines 171-177 as below.

$$g_s = \text{argmax}(A_{net} - A_{net}\frac{E}{E_{crit}}) \quad \text{Eq. (6)}$$

where E is the leaf-level transpiration rate, and E_{crit} is the critical transpiration rate at which the leaf xylem hydraulic conductance decreases to 0.1% of the maximum value (namely at 99.9% loss of hydraulic conductance). β does not directly scale stomatal conductance; instead, it is applied to hydraulic conductance, thereby influencing transpiration-driven water flow.

Table 1: Where is Vcmax?

[Response]

V_{cmax} is used in the calculation of net photosynthesis rate (A_{net}). Photosynthesis is solved by using both the Farquhar model and the diffusion model as below. This equation has been added into the revised clean version as Eq. 1.

$$A_{net} = V_{cmax}\frac{C_i - \Gamma^*}{C_i + K_m} - R_d = g_s \cdot (C_a - C_i) \quad \text{Eq. (1)}$$

V_{cmax} is the maximum rate of Rubisco activity and K_m is the Michaelis-Menten coefficient for Rubisco kinetics. Γ* is the CO_2 compensation point in the absence of dark respiration and R_d is the dark respiration rate. C_a is ambient CO_2 concentration. C_i is the intercellular CO_2 concentration.

Line 229: just curious. Why 63% instead of 50%?

[Response]

The classical Weibull cumulative distribution function (CDF) is

$$F(x) = 1 - e^{-(\frac{x}{\beta})^k}$$

where β is a scale parameter. k is a shape parameter. If we evaluate it at x=β, $F(\beta)=1-e^{-1}\approx 0.632$. The scale parameter corresponds to the point where the cumulative probability reaches ~63.2%. When mapping to hydraulic vulnerability curve, PLC is computed as:

$$\frac{K}{K_{max}} = e^{-(\frac{-\psi}{b})^c}$$

$$PLC = 1 - \frac{K}{K_{max}} = 1 - e^{-(\frac{-\psi}{b})^c}$$

This is mathematically identical to the Weibull CDF.

When $|\psi|==b$, $PLC=1-e^{-1}\approx0.632$

Figure 1b): would be great to show the related equations to better understand this figure. Also see the first major comment.

[Response]

The equations related to Figure 1b are shown here. They have been included in Methods (Section 2.3-2.6) in the revised clean version.

$$K = K_{max} \cdot e^{-1 \cdot (\frac{-\psi}{b})^c}$$

K_{max} is maximum hydraulic conductance. b and c are empirical parameters. ψ is leaf water potential.

$$T = \sum_{i=1}^{n_{canopy}} 1.6 \cdot g_s \cdot D \cdot LAI_i$$

LAI_i is the leaf area index of i^{th} layer. 1.6 is the unitless relative diffusivity of water vapor with respect to CO_2.

$$\psi_{leaf} = \psi_{soil} - F \times \sum_{i \in leaf,stem,root} \frac{1}{K_i}$$

F is transpiration-driven vertical water flow. K_i is hydraulic conductance of each segment. Ψ_{soil} is soil water potential.

Figure 4: Why is the difference between RMSEFR in b and c so large? They should be based on the same model without β, right?

[Response]

Under full recovery (FR) assumption, β was included and applied to different locations. Panel (b) and (c) used the same Medlyn stomatal model but applied β to either V_{cmax} or g1 part. Applying β to V_{cmax} represents a biochemical limitation, directly reducing photosynthetic capacity and indirectly constraining stomatal conductance through reduced assimilation. This formulation leads to a stronger and more persistent reduction in GPP, with comparatively weaker impacts on transpiration. In contrast, applying β to g1 represents a non-biochemical (stomatal) limitation,

directly reducing stomatal conductance and CO_2 diffusion, thereby suppressing transpiration and secondarily reducing photosynthesis. This means when model performance on transpiration is similar between two setups, which was the case here as transpiration was used in the error function to optimize K_{max}, photosynthesis in Medyn-g1 would be slightly higher than that in Medlyn-V_{cmax}. These two parameterizations therefore produce distinct responses of carbon and water fluxes under drought and during recovery as shown in Figure 4. To address this issue, we have added the below explanation in lines 325-332 in the revised clean version.

> These contrasting performances can be explained by the representations in the two model setups. Applying β to V_{cmax} represents a biochemical limitation, directly reducing photosynthetic capacity and indirectly constraining stomatal conductance via reduced assimilation. This leads to a stronger and more persistent reduction in GPP, with comparatively weaker impacts on transpiration. In contrast, applying β to g1 represents a non-biochemical (stomatal) limitation, directly reducing stomatal conductance and CO_2 diffusion, thereby suppressing transpiration and secondarily reducing photosynthesis. As a result, when model performance of transpiration is similar between the two setups, as in the FR scenario, where transpiration is used to constrain K_{max}, photosynthesis simulated by the Medyn-g1 tends to be slightly higher than that from the Medlyn-V_{cmax} configuration (Figure 5b, 5c).

Lines 384-390: see the 3rd major comment.

[Response]

We conducted additional model simulations using observation-based partitioned transpiration as a constraint. The results do not change our conclusion that delayed recovery can be effectively captured by incorporating biochemical limitations.

Lines 484-485: see the 3rd major comment.

[Response]

We agree with the Reviewer that soil evaporation may compensate for reduced transpiration, potentially leading to a rapid recovery of ET. To account for this, we used observation-based partitioned transpiration as a constraint and repeated the model simulations. We find that during

the recovery period, the full-recovery scenario overestimates both GPP and transpiration, although this does not alter our conclusion that incorporating biochemical limitations helps resolve the model-observation mismatch. We have therefore removed the description "quick resumption of ET" from the manuscript.

Lines 488-489: From my understanding, under the partial recovery scenario, the model needs to be calibrated by observations during the recovery phase. Would this prevent it from applying to the case where the observation is not available?

[Response]

Yes, calibrating the model against observations is required to optimize its ability to capture the extent of partial recovery. Regarding generalizability, the proposed method can be applied at sites with eddy-covariance observations to derive general constraints on vegetation recovery processes, which can then be transferred to sites lacking eddy-covariance measurements. For example, key recovery characteristics, such as the time required for the release of accumulated water deficit and the upper bound of hydraulic conductance recovery, can be derived from existing eddy-covariance observations. These features can then be related to commonly available environmental variables using nonlinear regression or machine-learning approaches, enabling their prediction at sites without eddy-covariance data. We have discussed this potential application in lines 449-456.

> This site-level research lays the groundwork for potential regional expansions to delve further into the factors influencing drought recovery and to validate the generalizability of the identified responses. Specifically, the proposed approach can be applied at sites with eddy-covariance observations to derive general constraints on vegetation recovery processes, which can then be extended to sites lacking such measurements. For example, key recovery characteristics, such as the time required for the release of accumulated water deficit and the upper bound of hydraulic conductance recovery, can be inferred from flux tower data. These features can subsequently be linked to commonly available environmental variables using nonlinear regression or machine-learning approaches, enabling their prediction across broader spatial domains without eddy-covariance coverage.

References

Haberstroh, S., Christen, A., Sulzer, M., Scarpa, F., & Werner, C. (2025). Recurrent hot droughts cause persistent legacy effects in a temperate Scots Pine forest. Plant Biology. doi: 10.1111/plb.70066

Matusick, G., Ruthrof, K. X., Kala, J., Brouwers, N. C., Breshears, D. D., & Hardy, G. E. S. J. (2018). Chronic historical drought legacy exacerbates tree mortality and crown dieback during acute heatwave-compounded drought. Environmental Research Letters, 13(9), 095002.